Molecular Orientation and Deformation of Polymer Solutions under Shear: A Flow Light Scattering Study

Ellen C. Lee, Michael J. Solomon, and Susan J. Muller*

Department of Chemical Engineering, University of California, Berkeley, California 94720, and Center for Advanced Materials, Lawrence Berkeley National Laboratory, Berkeley, California 94720

Received May 19, 1997; Revised Manuscript Received August 25, 1997[⊗]

ABSTRACT: The conformational characteristics of polymer coils in dilute solution under shear flow were investigated by means of wide angle laser light scattering in an apparatus similar to one used by Cottrell, Merrill, and Smith (*J. Polym. Sci., Polym. Phys. Ed.* **1969**, *7*, 1415).[1] The polymer solution was subjected to steady, homogeneous shear flow in the annulus between concentric cylinders by rotation of the inner cylinder. By examining the angular dependence of the scattered light intensity during shear, the orientation and the lengths of the major and minor axes of the deformed polymer molecules in solution were determined quantitatively. The solutions studied were linear polystyrenes of various molecular weights dissolved in the viscous solvent dioctyl phthalate near the Θ temperature. The shear rate dependence of the orientation angle of the deformed molecules was found to agree well with Zimm model predictions. The elastic dumbbell, Rouse, and Zimm models, however, substantially overpredict the degree of deformation of the polymer coils. This is in agreement with results of Link and Springer (*Makromol. Chem., Macromol. Symp.* **1992**, *61*, 358; *Macromolecules* **1993**, *26*, 464.).[2,3] In addition, the effects of concentration, molecular weight, and polydispersity were systematically studied. The sensitivity of the coil deformation to concentration persisted to concentrations significantly below c^*. Polydispersity had a significant effect on both the measured orientation and the deformation of the polymer molecules; the molecular weight dependence of the deformation was weaker than predicted by the Zimm model.

Introduction

Knowledge of the conformation of isolated polymer molecules undergoing flow is essential to understanding the macroscopic flow behavior of polymeric liquids. Predictions of coil orientation and deformation under flow are available from a number of kinetic theory models, e.g., for Rouse and Zimm chains, but few experimental results regarding coil dimensions are available for comparison. While extensive bulk property measurements on polymer solutions are available, such as rheological material functions, the comparison of these data with kinetic theory predictions shows a number of discrepancies. Measurements of polymer coil dimensions under flow would provide a much more direct and fundamental test of kinetic theories. In addition, the dynamics of single chains are relevant to concentrated solution and melt behavior, since many theories for these systems incorporate single chain concepts.

Wide angle laser light scattering is ideal for this type of investigation. Because the size of the polymer molecules is on the order of the wavelength of the incident light, the scattered light exhibits angular dissymmetry. The dissymmetry is described by the form factor, or the particle scattering factor, and can yield the size and shape of the polymer coil in solution. Peterlin was the first to recognize the potential of light scattering in the determination of molecular conformation of polymer molecules under an imposed flow.[4,5] At about the same time, Heller showed similar calculations supporting the use of light scattering for these types of measurements.[6,7] Soon after, several other researchers tested these flow light scattering techniques using suspensions of rodlike particles,[8−10] and finally using polymer solutions.[1,11] Cottrell, Merrill, and Smith performed experiments on solutions of fractionated samples of polyisobutylene (of fairly narrow molecular weight distribution) in decahydronaphthalene and found that the orientation angles measured were in the range predicted by kinetic theory models. The deformations measured, however, were much smaller than model predictions.

Recently, interest in this approach was renewed and a few investigators have started to study flow light scattering of various polymer solutions in shear[2,3,12−15] and elongational[16] flows. Springer and co-workers have, to date, performed the most complete set of experiments on coil conformation by flow light scattering techniques. In 1984, Wölfle and Springer[14] constructed an apparatus that allows measurement of all three axes of the polymer coils independently. Using this apparatus, Link and Springer and co-workers[2,3] showed that, as expected, the dimension of the deformed chains in the neutral direction remains unchanged from equilibrium dimensions. In these works, they found that the orientation of the macromolecules in various viscous solvents is in the range predicted by kinetic theory models. In addition, although the trend was not followed strictly, increasing solvent quality was found to increase the degree of alignment with the flow direction. This is in agreement with findings of Zisenis and Springer in 1994.[13] While most of the work done by Springer and co-workers focuses on the orientation of macromolecules in shear flow, they do show that, for a single sample of polystyrene of molecular weight equal to 10.3×10^6, the deformation in shear is substantially lower than kinetic theory predictions.[2,3] This is in agreement with the earlier findings of Cottrell et al.

Another method commonly used to extract orientation and size information is birefringence. As discussed by Bossart and Öttinger,[17] orientation information obtained from birefringence and light scattering is complementary because of the difference in origin of the two effects. Using birefringence, one can measure the average local orientation of segments of the polymer

[⊗] Abstract published in *Advance ACS Abstracts,* November 1, 1997.

S0024-9297(97)00694-3 CCC: $14.00

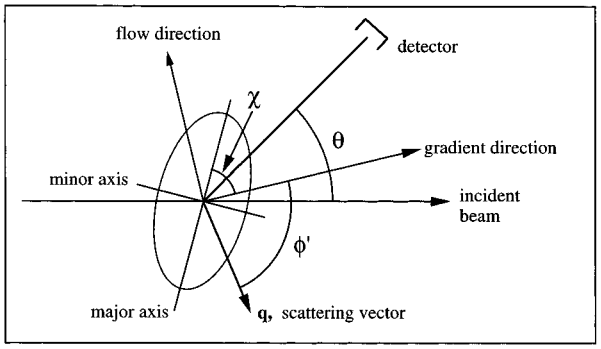

Figure 1. Shape of a deformed polymer coil in a shear flow, showing the major and minor axes, as well as the velocity and gradient directions. The orientation angle, χ, and the flow plane angle, ϕ', are shown for specific (arbitrary) detector and shear cell positions.

chain, rather than the overall orientation of the macromolecule. The relationship between birefringence and coil conformation is straightforward only in the absence of form birefringence and for small deformations from the equilibrium conformation (where chain statistics remain Gaussian). Conformational information from light scattering, on the other hand, arises from the gyration tensor. A direct measurement of a projected radius of gyration onto the detector can be obtained, so light scattering methods are not inherently limited to small deformations of the molecule.

Here, we present results from light scattering studies on several polymer solutions undergoing steady shear in circular Couette flow. The fluids are dilute solutions of polystyrene of various molecular weights dissolved in the viscous solvent dioctyl phthalate. Using the flow light scattering technique, we are able to measure quantitatively the orientation angle as a function of shear rate. Then, with the use of a Zimm-plot-type analysis, we also show quantitative determination of the polymer coil deformation. Both of these measures as a function of shear rate are compared to several kinetic theory models. Finally, because of the importance of polydispersity, molecular weight, and concentration effects to the processing of polymeric materials, and as a further test of predictions, we have examined the effects of these variables on the orientation and deformation of isolated polymer chains in steady shear flow.

Theory

The time-averaged shape of a polymer chain in quiescent solution is spherical due to rotational diffusion. When the magnitude of the shear rate exceeds the rate of rotational diffusion, however, the polymer chain deforms into an ellipsoidal shape and aligns to some degree with the direction of flow. One should see an increase in the coil dimension aligned in the direction of flow, a decrease in coil dimension in the direction of the gradient, and a constancy in the dimension in the neutral direction (see Figure 1), all of which can be measured by examining the scattered light. These deformed dimensions can be described by defining major, minor, and neutral axes of the polymer coil. The degree of alignment can be described by the orientation angle, χ, defined as the angle between the gradient direction and the major axis of the deformed polymer coil, such that $\chi = 90°$ indicates complete alignment with the flow. Note that this definition of χ is consistent with Cottrell et al.,[1] but that many authors, including Link and Springer,[2,3] define χ with respect to the flow direction rather than the gradient direction.

From light scattering theory, it is known that as the size of the scatterer increases, the destructive interference also increases, and thus the intensity is attenuated. As shown by Peterlin,[4] the intensity of light in the flow plane for an oriented polymer molecule should increase as the projected axis dimension decreases and show a maximum corresponding to the minor axis dimension of the polymer coil. Similarly, a minimum in intensity corresponding to the major axis dimension should occur (see Figure 3). The distribution of the intensity changes with the dimensionless shear rate as shown, with the orientation angle aligning more closely with the flow direction as the shear rate increases. In the limit of zero shear, the orientation angle approaches a value of $\chi = 45°$. From the scattering intensity distribution and the geometry of the setup, a measurement of the orientation angle can be obtained.

The elastic dumbbell, Rouse, and Zimm kinetic theories predict the orientation angle, χ, will vary with the shear rate in the following way:

$$\chi = 45° + \frac{\tan^{-1}(\beta/m)}{2} \tag{1}$$

where β is the dimensionless shear rate given by

$$\beta = \lambda\dot{\gamma} = \frac{[\eta]_0\eta_s M}{RT}\dot{\gamma} \tag{2}$$

λ is the characteristic relaxation time of the polymer molecules in solution, $[\eta]_0$ is the intrinsic viscosity, η_s is the solvent viscosity, M is the molecular weight of the polymer, $\dot{\gamma}$ is the shear rate, and R and T have their usual meanings. m is known as the orientation resistance of the molecule with the following values for light scattering:[17]

$$m = 1.0 \text{ for the elastic dumbbell model}$$

$$m = 1.75 \text{ for the Rouse model}$$

$$m = 2.553 \text{ for the Zimm model}$$

The magnitudes of the maxima and minima of the intensity curves give an indication of the deformation of the polymer coils. The major, minor, and neutral axes of the deformed molecule can be characterized by extension ratios defined in the following way:

$$e_i = \sqrt{\frac{\langle r_i^2\rangle_\beta}{\langle r_i^2\rangle_0}} \qquad i = \text{a, b, c} \tag{3}$$

where e_a is the major axis extension ratio, e_b is the minor axis extension ratio, e_c is the neutral axis extension ratio, $\langle r_i^2\rangle_\beta^{1/2}$ is the deformed chain major, minor, or neutral axis dimension, and $\langle r_i^2\rangle_0^{1/2}$ is the corresponding axis dimension in quiescent solution. An overall expansion ratio, e, of the polymer chain can also be calculated from the three axes extension ratios as

$$e = \sqrt{\frac{e_a^2 + e_b^2 + e_c^2}{3}} = \sqrt{\frac{\langle r_g^2\rangle_\beta}{\langle r_g^2\rangle_0}} \tag{4}$$

where $\langle r_g^2\rangle^{1/2}$ is the radius of gyration given by the following equation:

$$\langle r_g^2\rangle = \langle r_a^2\rangle + \langle r_b^2\rangle + \langle r_c^2\rangle \tag{5}$$

Table 1. Manufacturers' Data for Polystyrene Standards

sample	M_w	M_w/M_n
900k	9.3×10^5	≤1.06
1.5M	1.5×10^6	≤1.16
2M	1.9×10^6	≤1.30
3M	3.0×10^6	≤1.06
4M	3.9×10^6	≤1.06
6.5M	6.6×10^6	1.06
20M	2.0×10^7	≤1.30
10M (ref 3)	1.0×10^7	1.25

The overall expansion ratio is necessary to quantify the deformation of the polymer molecule because the three axis dimensions would still show an increase, decrease, and constancy if there were orientation but no deformation.

A quantitative measure of the size of the polymer coils can be obtained from the particle scattering factor through a Zimm-plot-type analysis, by which the projected axis dimension in the direction of the detector is determined from the slope of the data extrapolated to zero concentration. Both orientation angle and extension ratio determination are described in detail in Cottrell et al.[1]

The elastic dumbbell, Rouse, and Zimm predictions for deformation of the polymer coil can be expressed as

$$e^2 = 1 + \frac{2}{3m}\beta^2 \tag{6}$$

where the orientation resistance m and the dimensionless shear rate β are as defined above.

Experimental Section

Materials. Nearly monodisperse polystyrene (PS) standards of the following nominal molecular weights were obtained from Pressure Chemical: 9×10^5, 1.5×10^6, 2×10^6, 3×10^6, 4×10^6, and 2×10^7 (denoted by 900k, 1.5M, 2M, 3M, 4M, and 20M, respectively); and a 6.5×10^6 (denoted by 6.5M) nearly monodisperse standard was obtained from Polymer Laboratories. Manufacturers' data for weight average molecular weights (M_w) and polydispersity indices are given in Table 1. Samples of higher polydispersity were prepared by mixing various nearly monodisperse standards according to Table 2. Weight average molecular weights were measured by static light scattering, and polydispersity indices of the polydisperse mixtures were measured both by gel permeation chromatography and static light scattering.

The solvent used was dioctyl phthalate (DOP), which was chosen to match the refractive index of the shear cell and is a near Θ solvent for polystyrene at 25 °C. The physical properties of DOP at 25 °C are refractive index $n_D = 1.4860$, viscosity $\eta_s = 61$ cP. An index matching fluid, decahydronaphthalene (decalin), with a refractive index of $n_D = 1.475$ at 25 °C, was used in the light scattering vat to reduce or eliminate reflection and refraction of the laser beam at the glass/liquid interfaces. The decalin and DOP were obtained from Aldrich Chemical.

Solutions of polystyrene in DOP were prepared to concentrations ranging from $0.01c^*$ to $0.165c^*$, where c^* is the overlap concentration, obtained from the reciprocal of the intrinsic viscosity. The intrinsic viscosity of PS in DOP at 25 °C is given by the Mark−Houwink relation, $[\eta]_0 = KM^a$, with $K = 4.25 \times 10^{-4}$ dL/g and $a = 0.54$.[3] For the static light scattering measurements, the refractive index increment of these solutions was measured on a Brice-Phoenix differential refractometer equipped with a mercury arc lamp (Model BP-2000-V) to be $dn/dc = 0.1095$ mL/g at 25 °C. The second virial coefficient for the PS solutions was found to be $A_2 = 3.5 \times 10^{-5}$ cm^{3}mol/g^2. These are consistent with the values reported by Link and Springer.[3]

Sample Preparation. Samples for light scattering were prepared carefully in order to ensure dust-free solutions. The polymers were first dissolved in tetrahydrofuran (THF) and filtered through PTFE syringe filters with pore sizes of 0.45 μm (Gelman) for lower molecular weight polymers and 1.0 μm (Whatman) for higher molecular weight polymers. The clean solutions were then placed in a vacuum oven to volatilize the solvent in order to obtain dry, dust-free polystyrene. DOP was then filtered in through PTFE syringe filters with pore sizes of 0.2 μm (Gelman). The samples were examined by gel permeation chromatography (GPC) before and after filtering, and also after shearing experiments, to confirm that no shear degradation had occurred.

Gel Permeation Chromatography Apparatus. Characterization of the molecular weight distributions of the polymer samples was performed on a gel permeation chromatography system equipped with two on-line detectors, a Waters differential refractive index detector, and a Viscotek differential viscometer. The separation of molecular weights between 9×10^4 and 2×10^7 was achieved using three Styragel columns. The carrier solvent in the GPC system was THF, obtained from EM Science.

Light Scattering Apparatus. Static light scattering experiments were performed in a Brookhaven Instruments light scattering system, consisting of a goniometer equipped with a stepper motor and a photomultiplier tube. The incident light source was an Innova 70-2 argon ion laser with wavelength $\lambda_0 = 488$ nm. A temperature bath with a circulator regulated the temperature of the index matching vat and sample cell holder to within ±0.1 °C. Samples were prepared in clean Pyrex tubes of 13 mm nominal diameter.

The flow light scattering apparatus used for the shear experiments is a modification of the Brookhaven light scattering system (see Figure 2a). Modifications made to the system were similar to those of Cottrell et al.[1] The sample cell holder of the Brookhaven system was removed and a coaxial cylinder Couette shear cell was attached and immersed in the index matching vat filled with decalin. The shear cell was suspended from the top by two translation stages in order to allow movement of the cell with respect to the scattering volume of the light scattering system. The shear field was imparted on the polymer solution in the annulus of the shear cell by rotation of the inner cylinder driven by a computer-controlled stepper motor.

Both inner and outer cylinders of the shear cell were constructed of Corning 7740 glass, which was chosen for refractive index considerations ($n_{D,glass} = 1.474$; $n_{D,decalin} = 1.475$; $n_{D,DOP} = 1.486$). The inner cylinder is solid glass of diameter 30 mm and is attached to a stainless steel shaft at the top. The outer cylinder has an inner diameter of 33 mm and is closed on the bottom with an anodized aluminum cap.

Flow Light Scattering. The flow light scattering experiments were performed by measuring the intensity of scattered light in the flow plane, i.e., the plane containing the flow direction and the gradient direction. In our experimental setup, the flow plane and the Zimm plane (the plane containing the scattering vector and the primary beam) coincide, allowing independent measurement of only two coil dimensions. A schematic of the apparatus geometry is shown in Figure 2b. Alignment of the shear cell and the observed scattering volume were verified by performing an $I\sin\theta$ test with DOP (a Rayleigh scatterer) in the cell. The slight refractive index mismatch between the cell and the solvent contributed only nominal angular dependence. The scattering angle was varied from $20° < \theta < 140°$ by the rotation of the photomultiplier tube mounted on a goniometer arm, which gives a scattering vector range of 6.6×10^{-3} nm$^{-1} < |\boldsymbol{q}| < 36 \times 10^{-3}$ nm^{-1}. Variation of the angle ξ (see Figure 2b) was achieved by translation of the entire Couette shear cell relative to the scattering volume and allowed the flow plane angle ϕ' (the angle between the gradient direction and the scattering vector) to be varied from $0° < \phi' < 180°$, independent of θ. Since a maximum in the projected dimension of the polymer molecules corresponds to a minimum in intensity, a variation of ϕ' at constant θ then allows for the determination of the orientation angle, χ.

Once the orientation angle as a function of shear rate is determined, the deformation of the molecules can be measured by a Zimm-plot-type analysis. In a Zimm-plot analysis of a

Table 2. Polydisperse Samples Constructed from Monodisperse Standards of Various Molecular Weights[a]

sample	900k (wt %)	1.5M (wt %)	2M (wt %)	3M (wt %)	4M (wt %)	6.5M (wt %)	$10^{-6}M_w$	M_w/M_n
2M/3M/4M			40	20	40		3.2	1.27
900k/3M	29			71			2.6	1.21
1.5M/4M		35			65		3.0	1.3
1.5/6.5M		64				36	3.1	1.55

[a] M_w and polydispersity index (M_w/M_n) values measured using static light scattering techniques.

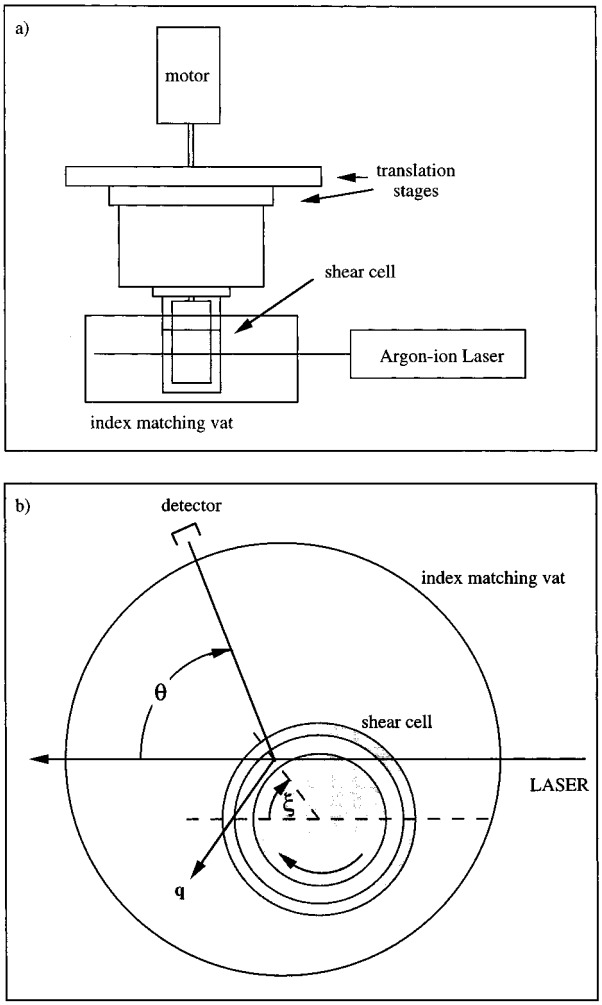

Figure 2. Flow light scattering apparatus: (a) side view; (b) top view. θ is the detector position in the Zimm plane, ξ is the shear cell position within the vat in the flow plane, and **q** is the scattering vector.

quiescent polymer solution, intensity data are collected at a series of detection angles θ at several concentrations, and radius of gyration, second virial coefficient, and molecular weight information are obtained by performing a double extrapolation to zero angle and zero concentration. The measurement of the deformation in a sheared solution requires determination of the projected dimensions of both the major and minor axes. The scattered light intensity is measured as a function of detection angle θ at constant ϕ' for $\phi' = \chi$ and $\phi' = \chi + 90°$ to obtain the major and minor axis dimensions. A strict and complete analysis of the coil dimensions and virial coefficient, as for the quiescent case, requires performing an extrapolation of concentration and detection angle data, respectively. For the quiescent Zimm plots of lower molecular weight samples, intensity measurements were typically taken in the range $40° < \theta < 140°$. For high molecular weight samples (20M and 6.5M), however, intensity measurements were taken at $20° < \theta < 90°$ due to curvature in constant concentration data at the high angles. This curvature is due to the nonlinearity in the isolated coil particle scattering factor.

The shear data are obtained by measuring the intensity of light scattered by the solution in the shear cell both during shear and at rest. The ratio of the shear to quiescent intensities is then applied to the quiescent solution static light scattering data in order to construct the shear Zimm plot.[1] From the slope of the zero concentration extrapolated data, we can obtain two of the three polymer coil axis dimensions in the sheared solution. We assume that the third dimension (in the neutral direction) remains unchanged, and can thus calculate the overall chain expansion. The assumption of constancy in the neutral direction was confirmed by calculations by Wang[18] and experimentally by Link and Springer,[2,3] who were able to measure all three axis dimensions independently. Shear rates in all experiments were kept in the range $\beta \leq 5$ due to shear-induced phase separation exhibited by solutions of PS in DOP above $\beta = 5$ at 25 °C.[19–22]

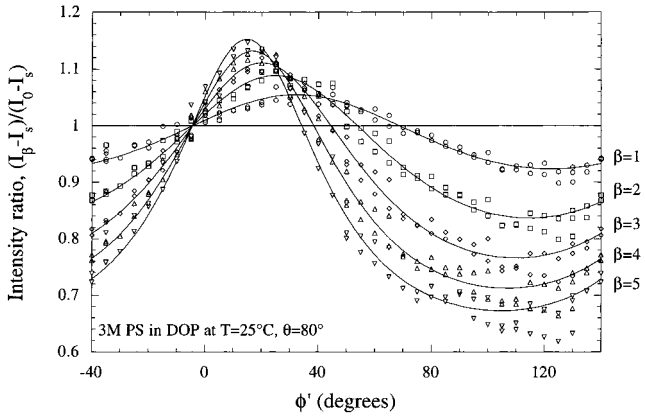

Figure 3. Intensity ratio, $(I_\beta - I_s)/(I_0 - I_s)$, in the flow plane for 3M PS in DOP at $T = 25$ °C, $\theta = 80°$.

Results

Orientation Angle. Figure 3 shows the intensity distribution in the flow plane at a fixed detection angle, θ, for a sample of 3M PS in DOP for increasing values of the dimensionless shear rate. The detector was set at $\theta = 80°$ since there was minimal reflection and refraction of the primary beam at this position. The intensity is plotted as a ratio, $(I_\beta - I_s)/(I_0 - I_s)$, where I_β is the scattering intensity of the sheared solution, I_s is the scattering intensity of the solvent alone, and I_0 is the scattering intensity of the quiescent solution. The maxima of the intensity curves indicate the angle of the major axis of the deformed polymer molecules, while the minima indicate the minor axis for the various shear rates. The orientation angle of the molecules is given by

$$\chi = 90° - \phi'_{max} \tag{7}$$

where ϕ'_{max} is the angle at which the intensity is a maximum. The maxima of the intensity curves were used in orientation angle determination because they are more sharply defined than the minima. Also shown on the plot are fits to the data for intensity ratios based on the ellipsoidal shape of the deformed polymer coils. The experimental data agree well with the expected shape, as predicted by Peterlin. The salient features of the scattering intensity distribution are the separation of the maxima and minima by 90°, the larger

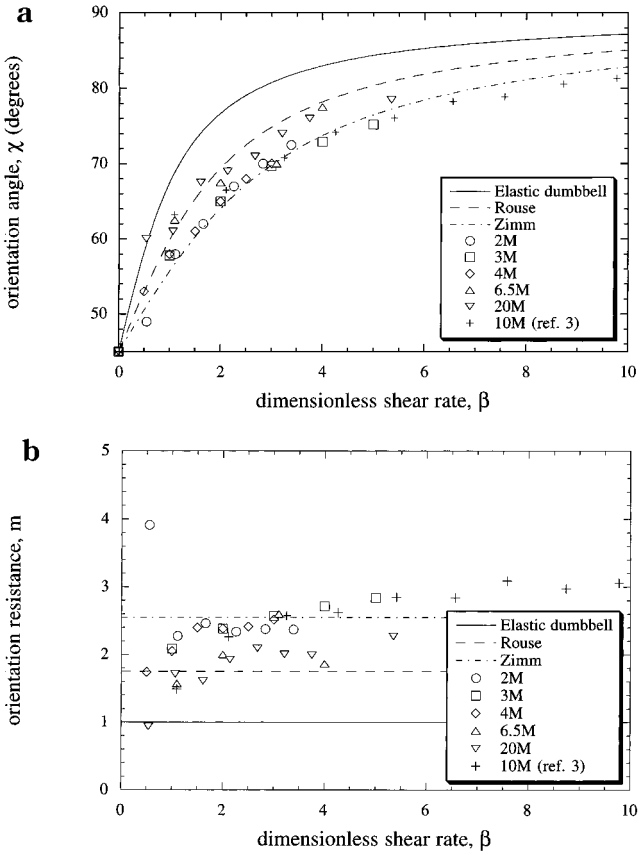

Figure 4. (a) Orientation angle, χ, versus dimensionless shear rate, β, with elastic dumbbell, Rouse, and Zimm model predictions. (b) Orientation resistance, m, versus dimensionless shear rate, β, with elastic dumbbell, Rouse, and Zimm model predictions. The data identified as "10M" are replotted from the work of Link & Springer[3] and are included for comparison.

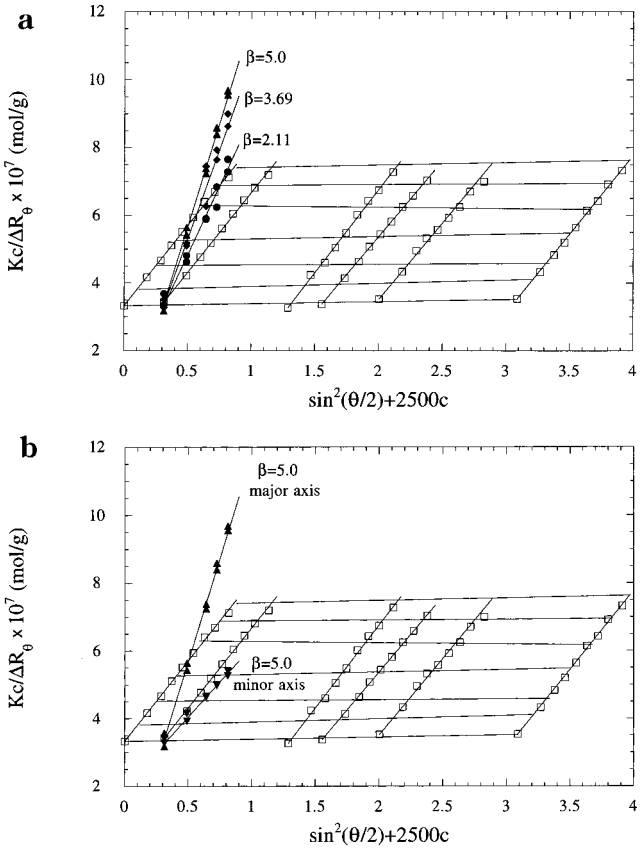

Figure 5. Sample Zimm plot of 3M PS in DOP at $T = 25$ °C. (a) Shear data at the major axis at three shear rates are superposed for a single concentration of $c = 0.017c^*$. (b) Shear data at major and minor axes at $\beta = 5.0$ are superposed for a single concentration of $c = 0.017c^*$.

change in the magnitudes of the minima than the maxima, and the crossing of all curves of varying β at a value of $\phi' = -5°$.

Figure 4a shows the orientation angles for the 3M PS sample calculated from Figure 3 as a function of the shear rate. Also shown are the orientation angles versus dimensionless shear rate β for the other molecular weight samples, obtained through experimental measurements similar to those shown in Figure 3. We have included in Figure 4a data from Link and Springer[3] for a 10.3×10^6 PS sample in DOP at 25 °C (denoted by 10M), as well as the elastic dumbbell, Rouse, and Zimm predictions. As expected, the orientation angle tends toward 90° as the shear rate increases, indicating more complete orientation with the direction of flow, and the orientation angle approaches a value of 45° as the shear rate approaches zero. Note also that data for all molecular weight samples overlay on scaling with the dimensionless shear rate β, in agreement with kinetic theory predictions. An alternative way to examine the data is to look at the orientation resistance as a function of shear rate (Figure 4b). This method of presenting the data emphasizes small departures from the models. The deviations in the measured orientation angles from the predictions at low β (≤ 1) are likely due to the inherent experimental difficulty in analyzing such small changes in the scattering intensity.

It is noted here that we do not examine the effect of concentration on the orientation of the polymer chains. Link and Springer[2,3] found a surprisingly strong effect of concentration on the orientation angle, where an increase in concentration increased the degree of alignment with the flow direction. The effect they observed, however, was limited to a range of rather high concentration ($0.75c^*$ to $0.3c^*$), and becomes negligible at concentrations below $0.15c^*$. From preliminary studies in our laboratory and from the data of Link and Springer, we find that the effects of concentration on orientation are negligible in the concentration range we have investigated.

Deformation. Once the orientation angle was determined for the polymer samples, it was possible to measure the deformation of the coils. Because of the good agreement between the experimental measures of the orientation angle and the Zimm model predictions, model values were used for cases in which we had no experimental data. In a sample plot, we show a quiescent solution Zimm plot for 3M PS in DOP with measured $M_w = 3.1 \times 10^6$, $\langle r_g^2 \rangle_0^{1/2} = 54.9$ nm, and $A_2 = 3.5 \times 10^{-5}$ (cm^3 mol)/g^2 (Figure 5a) with shear data taken at the major axis overlaid. The data here were obtained at various shear rates for a single concentration $c = 0.017c^*$. The slopes of the constant shear data lines are increased from those of the quiescent data, showing an increase in the major axis dimension from the equilibrium dimension. Note the slopes increase monotonically with shear rate. In Figure 5b, we show the same (3M PS in DOP) quiescent solution Zimm plot with shear data taken at both the major and minor axes overlaid for the single dimensionless shear rate $\beta = 5.0$. As expected, the minor axis shear data show a decrease in the slope, indicating a decrease in that dimension.

As mentioned previously, for a strict analysis of the deformed dimensions, data should be collected for

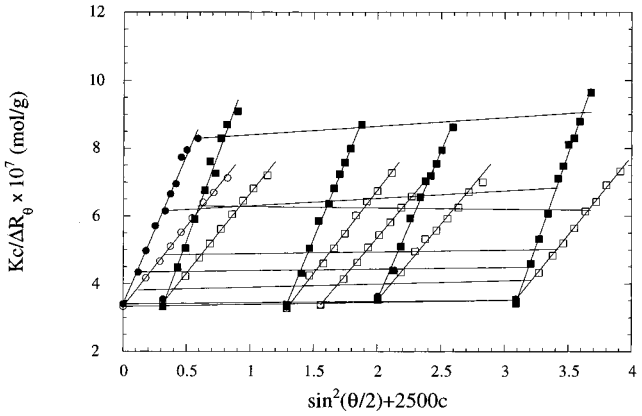

Figure 6. Zimm plot of 3M PS in DOP at $T = 25$ °C. Shear data are taken at the major axis for all concentrations at a single shear rate of $\beta = 3.17$.

several concentrations and extrapolated to zero concentration, with the projected dimensions of the deformed polymer coil obtained from the slope of the zero concentration extrapolated line. In Figure 6, we show a quiescent Zimm plot for the 3M PS sample with shear data taken at the major axis superposed for each concentration. The extrapolation of the shear data to zero concentration is also shown. From the ratio of the slopes of the shear data to the quiescent data, values for the major axis extensions were found for all concentrations. Minor axis extension ratios were determined in a similar manner. The overall expansion ratio, e, was then calculated from these values, assuming a neutral axis extension ratio of unity.[2,3] From the shear and quiescent Zimm plots of Figure 6 it is clear that the apparent A_2 in shear remains unchanged from quiescent conditions. Similar results have been found by other authors.[1,3,16] The intercept of the zero concentration shear data also remains unchanged in shear. We note that Menasveta and Hoagland observe a downward shift in the intercept, indicating an implausible increase in molecular weight, for solutions undergoing a strong extensional flow. Menasveta and Hoagland attribute this shift to the optical anisotropy that arises due to alignment of the phenyl groups of PS perpendicular to the flow direction on extension of the polymer molecules. Given the relatively small extension of the chains in the present shear flow, no shift is anticipated; the absence of any measurable intercept shift in shear is also consistent with the observations of Link and Springer.

Figure 7 shows overall expansion ratios calculated from the non-zero and zero concentration data. As the concentration is increased above $0.1c^*$, the overall chain expansion also increases. The concentration dependence is surprising, since all of the concentrations examined were well below c^*, where we expect isolated coil behavior. However, the result is consistent with the concentration dependence found by Link and Springer[2,3] for their 10M PS sample. Based on the data in Figure 7 where concentration effects appear negligible for concentrations below $0.1c^*$ (i.e., where the zero concentration limiting value of expansion ratio is recovered), all subsequent experiments were performed well below $0.1c^*$, and no extrapolations to zero concentration were then necessary. Also included in Figure 7 are various kinetic theory model predictions for the expansion ratio. In agreement with the earlier findings of Cottrell et al.[1] for their fractionated polyisobutylene samples and of Link and Springer[2,3] for the 10M PS sample, the deformation of the present 3M PS sample in DOP is

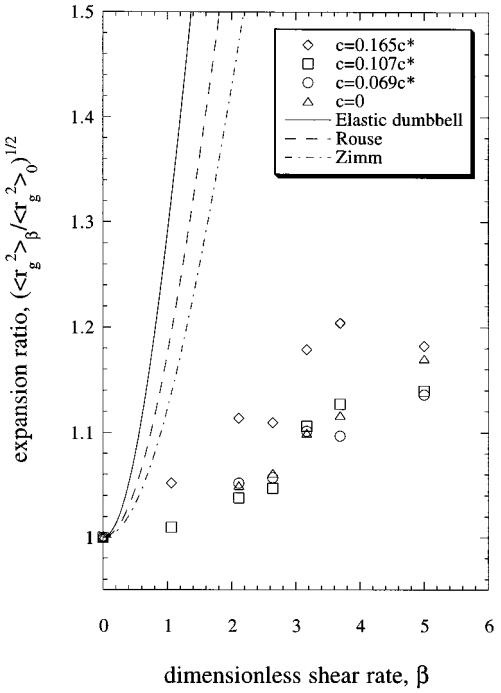

Figure 7. Effect of concentration on overall expansion ratio for 3M PS in DOP at $T = 25$ °C.

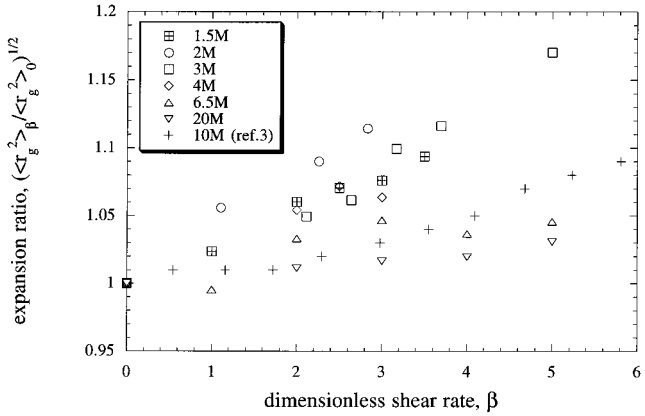

Figure 8. Overall expansion ratio, e, versus dimensionless shear rate, β, for all molecular weight samples at $T = 25$ °C. The data identified as "10M" are replotted from the work of Link and Springer[3] and are included for comparison.

substantially lower than elastic dumbbell, Rouse, and Zimm predictions.

To investigate the effect of molecular weight, the expansion ratio was measured for each of the nominally monodisperse polymers in solution; these data are shown in Figure 8. Contrary to the kinetic theory model predictions, the overall expansion ratio appears to be sensitive to molecular weight, with the smallest deformations measured for the highest molecular weight sample. Again, data from Link and Springer[3] for the 10M PS sample are included for the purposes of comparison; their data are consistent with the inverse (but not strict) dependence of the expansion ratio on molecular weight when plotted versus β. A possible explanation for the nonmonotonic molecular weight dependence may be related to differences in the polydispersities of the samples; this was investigated in the following set of experiments.

Polydispersity Effects: Sample Characterization. In order to address the effect of polydispersity, samples of varying polydispersity but similar weight

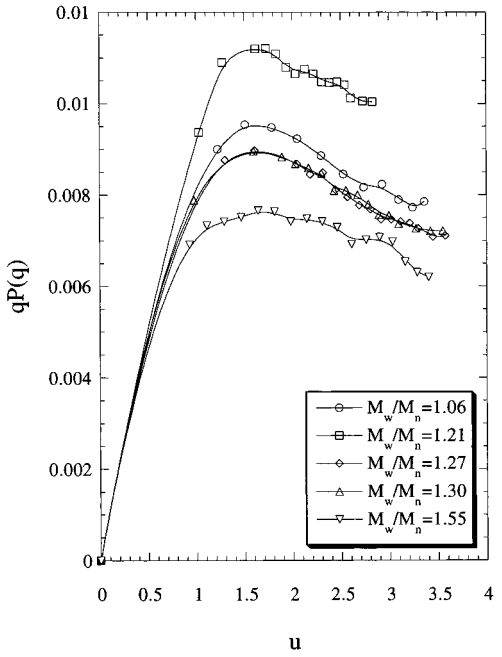

Figure 9. Bending rod plot for polydisperse samples. **q** is the scattering vector, $P(\mathbf{q})$ is the particle scattering factor, and $u = |\mathbf{q}|\langle r_g^2\rangle^{1/2}$. Positions of maxima indicate sample polydispersity. Lines are to guide the eye.

average molecular weight were prepared by mixing two or more monodisperse standards. The "recipes" are shown in Table 2; all of the polydisperse samples have $M_w \approx 3 \times 10^6$.

The weight average molecular weights of the polydisperse samples were measured using static light scattering techniques. The molecular weight distributions of the monodisperse standards and of the polydisperse samples were also checked by GPC. However, the polydispersity indices obtained from this size exclusion technique, even for the nearly monodisperse standards, were extremely sensitive to the choice of integration limits. Additionally, GPC is a secondary measurement of molecular weight, relying on calibration with the nearly monodisperse polymer standards. Therefore, a more direct method of polydispersity measurement was sought. In 1991, Denkinger and Burchard showed that static light scattering measurements could also be used in determining the chain stiffness and polydispersity of polymers in solution.[23] Using the bending rod plot and procedure outlined by these authors, we examined the polydispersity of each of the samples (see Figure 9) using only the static light scattering measurements. The resulting values for the polydispersity indices obtained assuming a Schulz−Zimm distribution are shown in Table 2; these values are in reasonably good agreement with a straightforward estimate based on the sample recipes and the assumption that the standards are monodisperse.

Polydispersity Effects on Orientation. Figure 10a shows average orientation angle versus shear rate for several polydisperse samples, and Figure 10b shows the corresponding orientation resistances from the same experiments. For increasing polydispersity, we observe an increase in the average orientation of the deformed molecules. This is consistent with predictions by Cottrell et al.[1] and with calculations by Bossart and Öttinger,[17] which indicate that the orientation resistance, m, should decrease for more polydisperse systems.

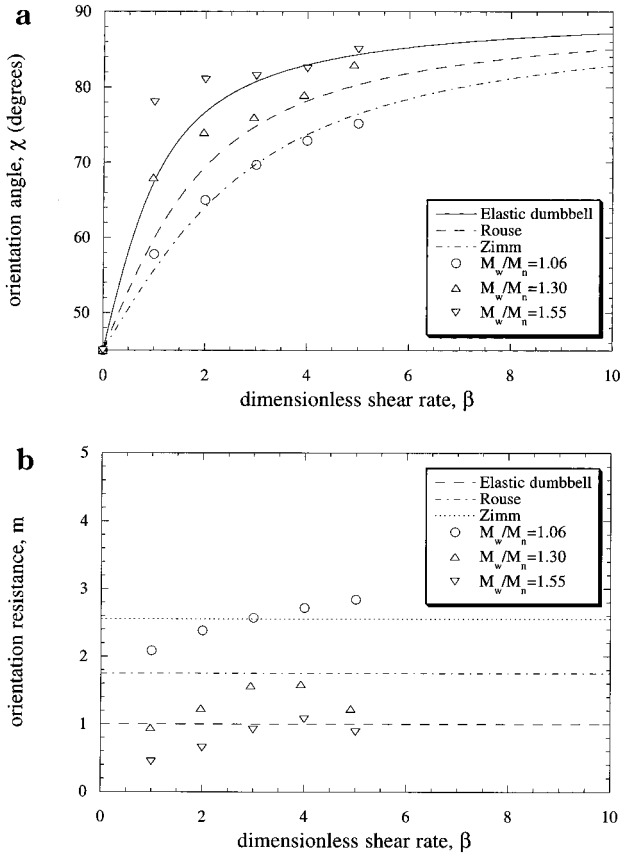

Figure 10. (a) Orientation angle, χ, versus dimensionless shear rate, β, for polydisperse samples. (b) Orientation resistance, m, versus dimensionless shear rate, β, for polydisperse samples.

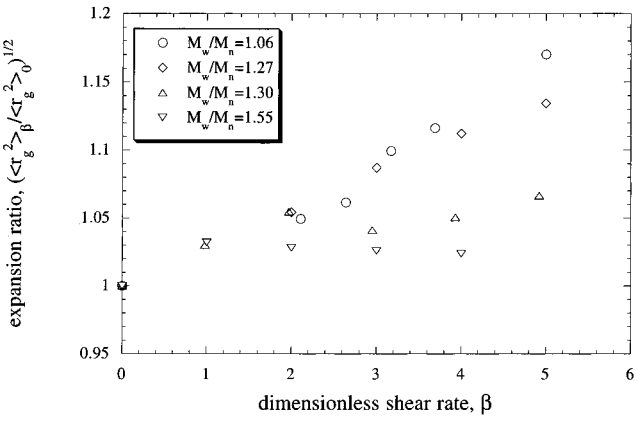

Figure 11. Overall expansion ratio, e, versus dimensionless shear rate, β, for polydisperse samples.

Polydispersity Effects on Deformation. Once the orientation behavior of a polydisperse sample was determined, the average polymer coil deformation of the polydisperse sample could be measured. The overall expansion ratio was found to decrease as the polydispersity of the sample increased, as shown in Figure 11. For a polydispersity index of $M_w/M_n = 1.55$, the expansion ratio is depressed nearly to unity; i.e., a fairly polydisperse sample shows essentially no measurable deformation. This trend is contrary to the predictions of Bossart and Öttinger.[17]

Discussion

In the present study, we have examined the light scattering from polymer solutions undergoing shear flow to obtain direct, quantitative measurements of the

resulting orientation and deformation of the macromolecules. The shear rates applied in these experiments correspond to $\beta \leq 5$. This constraint was imposed due to the shear-induced phase separation of PS/DOP solutions that occurs at $\beta > 5$ and has been extensively documented by others. Higher shear rates may be accessible in a better solvent for polystyrene, such as tricresyl phosphate, and studies in this solvent are currently underway.

Our present measurements, on nearly monodisperse polystyrenes of varying molecular weights in the near theta solvent dioctyl phthalate, have yielded a number of interesting results. The orientation angle measurements are consistent with those of others[1−3] and show no dependence on concentration c for the dilute solutions studied here, for which $c \leq 0.165c^*$. This latter result is also consistent with the experiments of Link and Springer. Our attempts to consider the effects of polymer molecular weight indicate that orientation angle data for all molecular weights appear to collapse to a single curve under appropriate scaling and are well described by the Zimm model predictions. In addition, we present for the first time measurements of the effects of polydispersity on orientation angle. As seen in Figure 10a, polydispersity effects on χ are substantial; our measurements are in qualitative agreement with the predictions of Bossart and Öttinger.[17] They found the orientation angle to be so sensitive to the polydispersity, in fact, that it was suggested that the polydispersity index could be calculated by a measurement of coil orientation, given the type of molecular weight distribution (i.e., Schulz−Zimm, log-normal, etc.) of the polymer sample.

The deformation or overall expansion ratio measurements are also consistent with the few experimental results available from earlier authors[1−3] and indicate that the elastic dumbbell, Rouse, and Zimm models substantially overpredict the expansion of a polymer in shear flow. The scaling of the overall expansion ratio e with shear rate β is approximately linear, as predicted, but the coefficient or slope is far lower than predicted. The origin of the discrepancies between the measured and predicted deformations remains unclear, but we note that even in extensional flow in the opposed jets geometry, as examined by Menasveta and Hoagland,[16] the deformation of the macromolecules is modest. These authors attribute the low deformability of the polymers in this strong flow to the short residence time of the polymer coils at the stagnation point, such that the total strain experienced by a single coil is quite small. While a limited residence time is not an issue in the steady, homogeneous shear flow we are investigating, our flow is weaker than a uniaxial extensional flow.

Also in agreement with the data of Link and Springer,[2,3] we find the measured expansion ratio increases with concentration for concentrations as low as $0.1c^*$, where single coil behavior is expected. One explanation for the persistence of the concentration sensitivity to such low values of c is that the polymer domains start to approach and overlap one another due to the expansion of the molecules under shear; however, we note that the expansion ratios measured under these conditions were not large enough to account for such overlap. Recently, Schneggenburger et al.[24] extended the FENE dumbbell theory to include concentration dependence in dilute polymer solutions that are well below the overlap concentration by including a mean-field term in the configurational distribution function. They show qualitative agreement of the extended model with the experimental data of Link and Springer.[3] Our data are also in qualitative agreement with the results of Schneggenburger et al.

In addition, as seen in Figure 8, the measured expansion ratios for different molecular weight samples do not collapse onto a single curve; that is, the coil deformation shows an unexpected molecular weight dependence when scaled with β. To gain further insight into this surprising result, we have investigated the role of polydispersity on deformation ratio. We find that increasing polydispersity results in a marked decrease in the measured expansion ratio; in fact, for $M_w/M_n > 1.55$, almost no coil expansion is measured even at the highest shear rate studied. While molecular weight effects remain somewhat unclear, the effects of polydispersity are consistent with a weaker dependence of coil expansion on both molecular weight and shear rate than the Zimm model predicts.

With respect to our finding of decreasing deformation with increasing polydispersity, we note that Cottrell et al. predicted the opposite dependence. Using the shear rate dependence of their narrowest sample as the monodisperse case, they calculated the expected expansion ratio for polydisperse samples by averaging all fractions of the samples' molecular weight distributions (assuming Schulz−Zimm distributions). These calculations show that the broader the sample, the higher the measured deformation. The effect of polydispersity comes into play through the dimensionless shear rate, β, in two ways. Each molecular weight fraction undergoes a different degree of alignment due to differing dimensionless shear rates. When the deformation measurement is then performed, an average value of the orientation is used, such that some fractions are not aligned properly with the detector position. This effect, which Cottrell et al. did not consider, always reduces the degree of deformation measured. The second effect of sample polydispersity comes about in the averaging of the degree of deformation of each of the molecular weight fractions. Each fraction will be deformed to a different extent due to (a) the different dimensionless shear rates experienced by the fractions and (b) any molecular weight dependence of the coil deformation not accounted for in β. The kinetic theory models considered here predict that this second effect results in an increase in the average deformation measured by light scattering techniques. As our experimental data indicate an inverse molecular weight dependence of the deformation, as well as a shear rate dependence that is significantly weaker than predicted, the averaging of monodisperse fractions in the broad samples results in a decrease in the measured deformation.

While it has been shown here that the Zimm model is capable of capturing several aspects of isolated polymer chain dynamics, its failure to predict the degree of deformation in shear indicates a serious shortcoming. The extreme sensitivity of chain deformation to molecular weight and polydispersity, however, may provide significant insight into how to better model polymer chain behavior.

Acknowledgment. This work was supported in part by the Director, Office of Energy Research, Office of Basic Energy Sciences, Materials Sciences Division of the U.S. Department of Energy under contract number DE-AC03-76SF00098. The authors also wish to acknowledge gifts to support polymer research from DuPont and Raychem.

References and Notes

(1) Cottrell, F. R.; Merrill, E. W.; Smith, K. A. *J. Polym. Sci., Polym. Phys. Ed.* **1969**, *7*, 1415.
(2) Link, A.; Zisenis, M.; Protzl, B.; Springer, J. *Makromol. Chem., Macromol. Symp.* **1992**, *61*, 358.
(3) Link, A.; Springer, J. *Macromolecules* **1993**, *26*, 464.
(4) Peterlin, A. *J. Polym. Sci.* **1957**, *23*, 189.
(5) Peterlin, A.; Heller, W.; Nakagaki, M. *J. Chem. Phys.* **1958**, *28*, 470.
(6) Heller, W. *Rev. Mod. Phys.* **1959**, *31*, 1072.
(7) Nakagaki, M.; Heller, W. *J. Polym. Sci.* **1959**, *38*, 117.
(8) Ahmad, N.; Heller, W.; Nakagaki, M. *J. Colloid Interface Sci.* **1969**, *31*, 585.
(9) Doppke, H. J.; Heller, W. *J. Colloid Interface Sci.* **1967**, *25*, 586.
(10) Okagawa, A.; Mason, S. G. *J. Colloid Interface Sci.* **1973**, *45*, 330.
(11) Champion, J. V.; Davis, I. D. *J. Chem. Phys.* **1970**, *52*, 381.
(12) Cleschinsky, D.; Stock, H.; Springer, J. *Colloid Polym. Sci.* **1991**, *269*, 1250.
(13) Zisenis, M.; Springer, J. *Polymer* **1994**, *35*, 3156.
(14) Wölfle, A.; Springer, J. *Colloid Polym. Sci.* **1984**, *262*, 876.
(15) Zisenis, M.; Springer, J. *Polymer* **1995**, *36*, 3459.
(16) Menasveta, M. J.; Hoagland, D. A. *Macromolecules* **1991**, *24*, 3427.
(17) Bossart, J.; Öttinger, H. C. *Macromolecules* **1995**, *28*, 5852.
(18) Wang, S.-Q. *J. Chem. Phys.* **1990**, *92*, 7618.
(19) Ver Strate, G.; Philippoff, W. *J. Polym. Sci., Polym. Lett. Ed.* **1974**, *12*, 267.
(20) Rangel-Nafaile, C.; Metzner, A. B.; Wissbrun, K. F. *Macromolecules* **1984**, *17*, 1187.
(21) Yanase, H.; Moldenaers, P.; Mewis, J.; Abetz, V.; van Egmond, J. W.; Fuller, G. G. *Rheol. Acta* **1991**, *30*, 89.
(22) van Egmond, J. W.; Fuller, G. G. *Macromolecules* **1993**, *26*, 7182.
(23) Denkinger, P.; Burchard, W. *J. Polym. Sci., Part B* **1991**, *29*, 589.
(24) Schneggenburger, C.; Kroger, M.; Hess, S. *J. Non-Newtonian Fluid Mech.* **1996**, *62*, 235.

MA9706945